

## Preparation and Photoelectrochemical Behavior of Cu<sub>2</sub>O/TiO<sub>2</sub> Inverse Opal Heterojunction Arrays

Hyun Sik Kim<sup>†</sup>, Sang Kwon Lee<sup>††</sup>, and Soon Hyung Kang<sup>††,\*</sup>

<sup>†</sup>School of Chemical & Biological Engineering, Seoul National University, Seoul 151-742, Korea

<sup>††</sup>Department of Chemistry Education, Chonnam National University, Gwangju 500-757, Korea

(Received June 26, 2012 : Accepted August 8, 2012)

**Abstract :** The Cu<sub>2</sub>O/TiO<sub>2</sub> inverse opal heterojunction arrays were developed by electrochemical deposition of Cu<sub>2</sub>O nanoparticles on TiO<sub>2</sub> inverse opal arrays. The Cu<sub>2</sub>O nanoparticles completely filled the inner pores of TiO<sub>2</sub> inverse opal film (prepared by liquid phase deposition with an average thickness of 400 nm) and covered the entire area; exhibiting high crystalline properties of anatase and cubic phase from TiO<sub>2</sub> and Cu<sub>2</sub>O, respectively. From asymmetric current-voltage profile, it was noticeable that a heterojunction was well formed for charge transport from Cu<sub>2</sub>O to TiO<sub>2</sub> film resulting from the enhanced charge separation yield. In addition, increased photocurrent of 0.19 mA/cm<sup>2</sup> (versus 0.08 mA/cm<sup>2</sup> under dark condition) was obtained at -0.35 V from the heterojunction structure in the 0.5 M Na<sub>2</sub>SO<sub>4</sub> solution.

**Keywords :** Inverse opal TiO<sub>2</sub>, Cu<sub>2</sub>O, Heterojunction, Photoelectrochemical behavior

### 1. Introduction

Nowadays, titanium dioxide (TiO<sub>2</sub>) is being widely investigated because of its photocatalytic, photoelectrochemical, and electrochromic properties as well as low cost, environmentally friendly material, and photostability in aqueous electrolytes.<sup>1-3)</sup> However, the rapid recombination of photoinduced electron hole pairs in TiO<sub>2</sub> greatly decreases its quantum efficiency in the photoelectrochemical (PEC) cells.<sup>4)</sup> Besides, the wide bandgap (3.2 eV) of TiO<sub>2</sub> absorbs only 5% of sunlight, thus limiting the exploration of widespread solar spectrum, including visible light. Therefore, several methods have been suggested to extend the light absorption towards visible wavelength. The first approach is the doping process in which the substitutional atoms are incorporated into the TiO<sub>2</sub> lattice, thus improving the visible light absorption.<sup>5)</sup> Ultimately, this approach has not been suitable for efficient photoelectrochemical or photocatalytic reactions due to the associated side reactions. The second is the

sensitization on the TiO<sub>2</sub> exploring organic dye or inorganic compounds (CdSe, CdS, and PbS etc.).<sup>6)</sup> Even though this method attains the high efficiency by the photocatalytic or photoelectrochemical applications, the stability of the cell in the aqueous electrolyte is never guaranteed due to occurrence of photocorrosion. Thus, one of the promising ideas to extend the light absorption of TiO<sub>2</sub> and to suppress the charge recombination reaction is to couple TiO<sub>2</sub> with narrow bandgap semiconductors with conformed band position. The well-combined heterojunction structure results in the fast charge separation because the photoinduced electrons are subsequently transferred from narrow bandgap semiconductor to TiO<sub>2</sub> with an increase in the lifetime of charge carriers from the retarded charge recombination reaction, thus enhancing the quantum yield.<sup>7)</sup> Considering the material stability and band matching at the interface to facilitate the carrier transfer, cuprous oxide (Cu<sub>2</sub>O), a *p*-type semiconductor is a fascinating material with a direct bandgap of 2.2 eV. Recently, Siripala *et al.* reported the formation of Cu<sub>2</sub>O/TiO<sub>2</sub> heterojunction thin film cathode for photoelectrocatalysis with high

\*E-mail: skang@jnu.ac.kr

efficiency for hydrogen production.<sup>8)</sup> In addition, Hou reported the fabrication of Cu<sub>2</sub>O/TiO<sub>2</sub> nanotube heterojunction arrays to demonstrate the enhanced charge separation yield.<sup>9)</sup>

Herein, we fabricated Cu<sub>2</sub>O/TiO<sub>2</sub> inverse opal heterojunction arrays by liquid phase deposition, followed by facile electrodeposition method. The 400 nm-sized TiO<sub>2</sub> inverse opal was found to supply sufficient surface area for direct contact to the photoactive Cu<sub>2</sub>O nanoparticles, probably leading to the high charge separation efficiency.

## 2. Experimental Details

### 2.1. Preparation of TiO<sub>2</sub> inverse opal film

Multilayer opal films were formed by slow gravimetric sedimentation of polystyrene (PS) colloidal particles with an average diameter of 400 nm onto fluorine doped tin oxide (FTO) substrate developed Nagayama *et al.*<sup>10)</sup> Above this substrate, the TiO<sub>2</sub> nanoparticles were filled into the inner space between the PS colloidal particles by liquid phase deposition. First, on the PS colloidal template, the seed layer should be formed to deposit the TiO<sub>2</sub> nanoparticles in solution containing 1.2 wt% titanium isopropoxide, 0.12 wt% HNO<sub>3</sub>, and ethanol as a solvent. The sample was vertically dipped for 5 min and subsequently held in air for 1 h. Afterwards, TiO<sub>2</sub> nanoparticles were deposited facilitating ammonium hexafluorotitanate as a precursor.) In order to develop TiO<sub>2</sub> inverse opal film, the removal of PS colloidal spheres is necessary and subsequently, this process should be performed by annealing process at 450°C for 8 h under air gas.

### 2.2. Cu<sub>2</sub>O deposition on the TiO<sub>2</sub> inverse opal film.

Electrochemical deposition was carried out exploring a potentiostat (Autolab84711) in a 3-electrode cell using the TiO<sub>2</sub> inverse opal film as a working electrode, a saturated Ag/AgCl electrode as reference, and a platinum wire as counter electrodes. The Cu<sub>2</sub>O was deposited potentiostatically at -0.38 V for 1 h with constant stirring in an electrolyte consisting of 0.35 M CuSO<sub>4</sub> and 3 M lactic acid (brought to pH 9 using 5 M NaOH).

Then, the bath temperature was maintained at 50°C during the deposition. At the termination of the experiment, the color of the sample changed from white to orange.

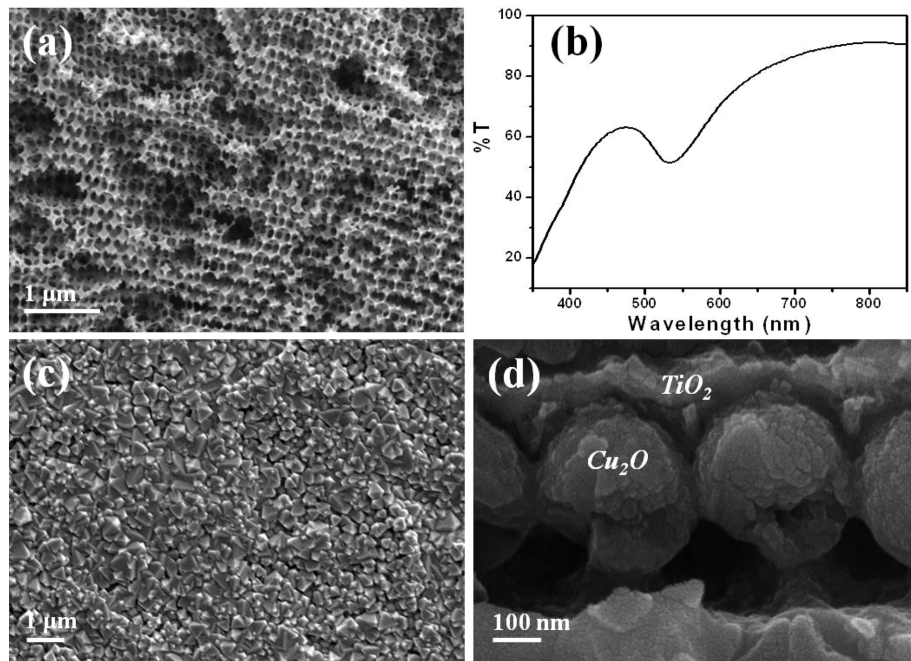
### 2.3. Characterization.

The *J-V* measurements were performed in the dark using a Keithley Model 2400. Graphite electrodes containing graphite flakes were painted on the surface of the films. The top graphite electrode served as the working electrode, while the bottom bare FTO substrate served as the counter/reference electrode. To check the TiO<sub>2</sub> inverse opal and Cu<sub>2</sub>O/TiO<sub>2</sub> heterojunction structure, a field-emission scanning electron microscope (FE-SEM, JEOL JSM-7000F) was employed. X-ray diffraction (XRD, Scintag DMS-2000 diffractometer using Cu K $\alpha$  radiation) was measured to confirm the crystallinity of the samples. The transmittance spectrum was obtained using a Shimadzu model 3100 UV-VIS spectrophotometer at a wavelength ranging from 350 nm to 850 nm. For the photoelectrochemical measurements, the same electrochemical configuration comprising of Cu<sub>2</sub>O/TiO<sub>2</sub> heterojunction film as working electrode, Pt wire as counter electrode, and saturated Ag/AgCl as reference electrode, respectively was facilitated in the electrolyte of 0.5 M Na<sub>2</sub>SO<sub>4</sub>. The Xe lamp (ABET Technologies, 100 mW/cm<sup>2</sup>) was irradiated onto the working electrode with actual geometric area of 1 cm<sup>2</sup> through the electrolyte.

## 3. Results and Discussion

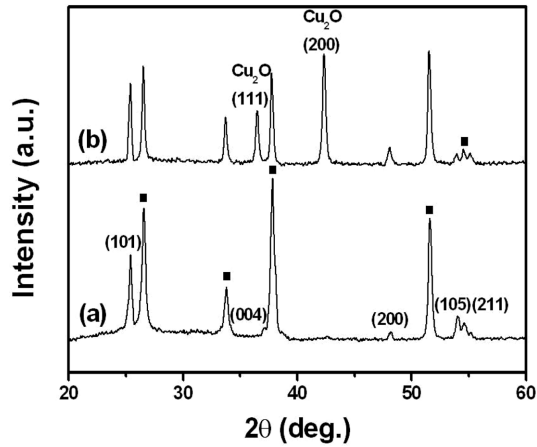
### 3.1. Characterization of TiO<sub>2</sub> inverse opal film and Cu<sub>2</sub>O/TiO<sub>2</sub> heterojunction film.

Fig. 1(a) shows FE-SEM images of the TiO<sub>2</sub> inverse opal film. It can be seen from the figure that the inverse opal structures are well ordered with 400 nm diameter particles arranged in a face-centered cubic lattice. In some parts of the sample, defects including cracks and vacancies are typically observed, attributed from film shrinkage during evaporative self-assembly of original PS colloidal template.<sup>11)</sup> In spite of this disorder, TiO<sub>2</sub> inverse opal film shows a photonic band gap (PBG) at position of 530 nm owing to Bragg reflection.<sup>12)</sup>



**Fig. 1.** FE-SEM images of (a) inverse opal  $\text{TiO}_2$  film, (b) UV-Vis transmittance of inverse opal  $\text{TiO}_2$  film, FE-SEM images of (c) surface and (d) cross-section view of  $\text{TiO}_2/\text{Cu}_2\text{O}$  heterojunction film on the FTO substrate.

Thus, a strong reduction in the transmittance in this position, with an increase in the absorbance of the sample was observed. Fig. 1(c) shows the surface morphology of  $\text{Cu}_2\text{O}/\text{TiO}_2$  heterojunction film. It can be seen in the figure that tetragonal-shaped  $\text{Cu}_2\text{O}$  nanoparticles have been deposited uniformly throughout the entire area of  $\text{TiO}_2$  inverse opal films. In particular, the top surface area is completely covered by  $\text{Cu}_2\text{O}$ . The result indicates that the  $\text{TiO}_2$  inverse opals never came in contact with graphite electrode in  $J-V$  measurement. Fig. 1(d) shows the cross-sectional view of  $\text{Cu}_2\text{O}/\text{TiO}_2$  heterojunction film. It is noticeable that the  $\text{Cu}_2\text{O}$  nanoparticles are infiltrated into the  $\text{TiO}_2$  inverse opal structure and covered through the surface area. This displays the well-formed  $\text{Cu}_2\text{O}/\text{TiO}_2$  heterojunction film with a thickness of approximately  $1.7 \mu\text{m}$  without any barrier or vacant space and shows the exploration of  $\text{TiO}_2$  inverse opals with large surface area. Actually, the thickness of used  $\text{TiO}_2$  inverse opals can be adjusted based on the thickness of PS colloidal film. However, the maximum thickness to form  $\text{Cu}_2\text{O}/\text{TiO}_2$  heterojunction film (within  $2 \mu\text{m}$ ) is



**Fig. 2.** XRD spectra of (a)  $\text{TiO}_2$  inverse opal film and  $\text{TiO}_2/\text{Cu}_2\text{O}$  heterojunction film.

controlled by  $\text{Cu}_2\text{O}$  because of the limited deposition thickness of  $\text{Cu}_2\text{O}$  materials by electrodeposition, attributable to the low electrical conductivity. Therefore, we used  $1.7 \mu\text{m}$  thick  $\text{Cu}_2\text{O}/\text{TiO}_2$  heterojunction film for the characterization and PEC test. Fig. 2 displays the XRD spectra of  $\text{TiO}_2$  inverse opal and  $\text{Cu}_2\text{O}/\text{TiO}_2$

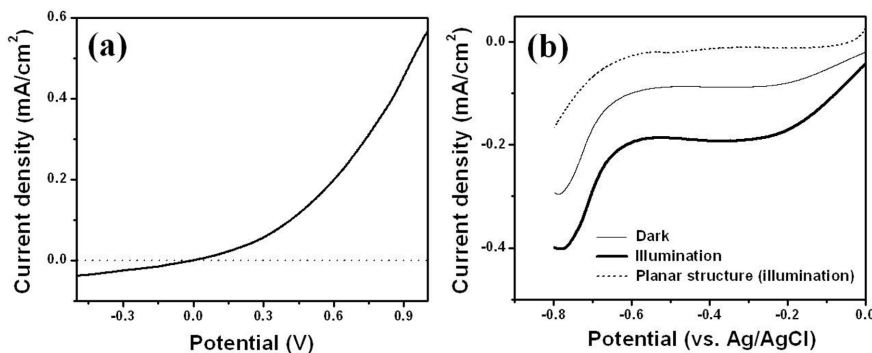


**Fig. 3.** *J-V* curves and photocurrent density of (a) TiO<sub>2</sub>/Cu<sub>2</sub>O/graphite heterojunction film.

heterojunction films on the FTO substrate. The XRD peak related to the substrate has been indicated by dotted line. The presence of the anatase (101) plane in the TiO<sub>2</sub> film can be clearly identified at 25.3°. In the case of Cu<sub>2</sub>O/TiO<sub>2</sub> film, all the peaks of Cu<sub>2</sub>O as well as TiO<sub>2</sub> can be well assigned to those of cubic phase with diffraction peaks at 2θ = 37.7 and 42.3°.<sup>13)</sup> This result reveals that the Cu<sub>2</sub>O and TiO<sub>2</sub> consisting of heterojunction exhibits the cubic and anatase phase, respectively.

### 3.2. Dark J-V and PEC properties of Cu<sub>2</sub>O/TiO<sub>2</sub> heterojunction film

Fig. 3(a) shows the dark *J-V* characteristics of Cu<sub>2</sub>O/TiO<sub>2</sub> heterojunction film in 2 electrode systems composed of graphite electrode as a top layer and FTO substrate as a bottom layer. Note that the dark current of TiO<sub>2</sub> inverse opal film is almost zero, which is not shown here. On the other hand, *J-V* curve of Cu<sub>2</sub>O/TiO<sub>2</sub> heterojunction film exhibits the asymmetric shape in the forward and reverse bias. An increase in current is observed with the positive bias reaching to 0.14 mA/cm<sup>2</sup> at 0.5 V, while a decrease is observed with negative bias as -0.04 mA/cm<sup>2</sup> at -0.5 V. The change in asymmetric current under forward and reverse bias directions indicates rectifying behavior, demonstrating that the bilayer structure has a *p-n* junction property and forms the heterojunction constituted of TiO<sub>2</sub> inverse opal and Cu<sub>2</sub>O film. Internal electric field formed in the heterojunction may suppress the charge recombination reaction at the junction region, inducing more surviving carriers from several side reactions to take part in the

redox reaction.<sup>14)</sup> Fig. 3(b) shows the current density of Cu<sub>2</sub>O/TiO<sub>2</sub> heterojunction film measured in dark and illumination condition using 0.5 M Na<sub>2</sub>SO<sub>4</sub> electrolyte. The dark current density is just 0.08 mA/cm<sup>2</sup> at 0.35 V, whereas that under condition of illumination is above 0.19 mA/cm<sup>2</sup>. To be precise, the heterojunction array showed photocurrent density as 0.11 mA/cm<sup>2</sup>. Such a high photocurrent implies the survival of more carriers in charge recombination reaction, resulting from the improved separation efficiency of photogenerated electrons and holes in Cu<sub>2</sub>O in the situation where the conduction band of Cu<sub>2</sub>O is -1.2 eV more negative than that of TiO<sub>2</sub>, and contributed to the enhancement of photocurrent in the heterojunction.<sup>15)</sup> Also, in order to assess the geometric effect, the planar structure Cu<sub>2</sub>O/TiO<sub>2</sub> heterojunction film prepared by the same experimental procedure was evaluated. As shown in the Fig. 3, it was seen that the photocurrent (0.01 mA/cm<sup>2</sup> at 0.35 V) is pretty low compared to that of 3-dimensional (D) inverse opal film, attributed from the specific surface area effect. Accordingly, it can be known that the constitution of the heterojunction array film using 3-D inverse opal film grants the large photocurrent by large surface area with the improved separation efficiency by forming the heterojunction. Note that the pure Cu<sub>2</sub>O material developed by the same experimental procedure showed the abrupt photocorrosion behavior under condition of illumination, giving rise to the low photocurrent density. However, the fabrication of Cu<sub>2</sub>O/TiO<sub>2</sub> heterojunction alleviates the photocorrosion issue because of the fast charge transfer to TiO<sub>2</sub> film.<sup>8)</sup>

#### 4. Conclusions

The Cu<sub>2</sub>O/TiO<sub>2</sub> inverse opal heterojunction was developed by the liquid phase deposition to make TiO<sub>2</sub> inverse opal film with an average diameter of 400 nm, followed by simple electrodeposition for Cu<sub>2</sub>O thin film. Approximately, 1.7 μm thick heterojunction shows the asymmetric J-V curve, demonstrating that internal electric field formed in the junction region suppresses the charge recombination reaction, offering more surviving carriers for photoelectrochemical reaction in 0.5 M Na<sub>2</sub>SO<sub>4</sub>.

#### Acknowledgments

This work was supported by the National Research Foundation of Korea Grant funded by the Korean Government (Ministry of Education, Science and Technology). (NRF-2011-0840) (SHK) Also, this study was financially supported by Chonnam National University, 2011.

#### References

1. B. O'Regan and M. Grätzel, 'A low-cost, high-efficiency solar cell based on dye-sensitized colloidal TiO<sub>2</sub> films', *Nature*, London, **353**, 737 (1991).
2. T. M. Wang, S. K. Zheng, W. C. Hao and C. Wang, 'Studies on photocatalytic activity and transmittance spectra of TiO<sub>2</sub> thin films prepared by r.f. magnetron sputtering method' *Surf. Coat. Technol.*, **155**, 141 (2002).
3. N. Janke and A. Bieberle, 'Characterization of sputter-deposited WO<sub>3</sub> and CeO<sub>2-x</sub>TiO<sub>2</sub> thinfilms for electrochromic applications' *Thin Solid Films*, **392**, 134 (2001).
4. S. C. Lo, C. F. Lin, C. H. Wu, P. H. Hsieh, 'Capability of coupled CdSe/TiO<sub>2</sub> for photocatalytic degradation of 4-chlorophenol' *J. Hazard Mater.*, **B114**, 183 (2004).
5. S. H. Kang, H. S. Kim, J. Y. Kim and Y. E. Sung, 'Enhanced photocurrent of nitrogen-doped TiO<sub>2</sub> film for dye-sensitized solar cells' *Mater. Chem. Phys.*, **124**, 422 (2010).
6. W. Lee, S. H. Kang, S. K. Min, Y. E. Sung and S. H. Han, 'Co-sensitization of vertically aligned TiO<sub>2</sub> nanotubes with two different sizes of CdSe quantum dots for broad spectrum' *Electrochim. Comm.*, **10**, 1579 (2008).
7. M. K. Lee and T. H Shih, 'High photocatalytic activity of heterojunction of zinc selenide grown on nano-scaled titanium oxide' *J. Electrochem. Soc.*, **154**, P49 (2007).
8. W. Siripala, A. Ivanovskaya, T. F. Jaramillo, S. Baek and E. W. McFarland, 'A Cu<sub>2</sub>O/TiO<sub>2</sub> heterojunction thin film cathode for photoelectrocatalysis' *Sol. Energy Mater. Sol. Cells*, **77**, 229 (2003).
9. Y. Hou, X. Y. Li, Q. D. Zhao, X. Quan and G. H. Chen, 'Fabrication of Cu<sub>2</sub>O/TiO<sub>2</sub> nanotube heterojunction arrays and investigation of its photoelectrochemical behavior' *Appl. Phys. Lett.*, **95**, 093108 (2009).
10. N. D. Denkov, O. D. Velev, P. A. Kralchevsky, I. B. Ivanov, H. Yoshimura and K. Nagayam, 'Mechanism of formation of two-dimensional crystals from latex particles on substrates' *Langmuir*, **8**, 3183 (1992).
11. N. V. Dziomkina and G. Julius Vancso, 'Colloidal crystal assembly on topologically patterned templates' *Soft Mater.*, **1**, 265 (2005).
12. R. C. Schrodin, M. Al-Daous and A. Stein, 'Self-modification of spontaneous emission by inverse opal silica photonic crystals' *Chem. Mater.*, **13**, 2945 (2001).
13. R.-M. Liang, Y.-M. Chang, P.-W. Wu and P. Lin, 'Effect of annealing on the electrodeposited Cu<sub>2</sub>O films for photoelectrochemical hydrogen generation' *Thin Solid Films*, **519**, 7191 (2010).
14. Y. Hou, X. Y. Li, X. J. Zou, X. Quan and G. H. Chen, 'Photoelectrocatalytic activity of a Cu<sub>2</sub>O-loaded self-organized highly oriented TiO<sub>2</sub> nanotube array electrode for 4-chlorophenol degradation' *Environ. Sci. Technol.*, **43**, 858 (2009).
15. J. Ghijssen, L. H. Tjeng, J. van Elp, H. Eskes, J. Westerink and G. A. Sawatzky, 'Electronic structure of Cu<sub>2</sub>O and CuO' *Phys. Rev. B*, **38**, 11322 (1988).